Compact Design of a Slotless Type PMLSM Using Genetic Algorithm with 3D Space Harmonic Method

Dong-Yeup Lee* and Gyu-Tak Kim*

Abstract - In this paper, in order to enhance thrust of slotless type Permanent Magnet Linear Synchronous Motor, an optimal design is achieved by combining a genetic algorithm with 3D space harmonic method. In the case of multi-objective functions, the ratio of thrust/weight and thrust/volume are increased by 7.56[%] and 7.98[%], respectively.
Thus, miniaturization and lightweight were realized at the same time.

Keywords: Slotless type PMLSM, Genetic Algorithm, 3D Space Harmonic Method, Multi-objective Function

I. Introduction

If a linear motor can be selected in the systems demanding high speed as well as high precision for both step-up in production and high quality, there are no friction and backlash in direct drive linear motors. Hence, a slotless type permanent magnet linear synchronous motor(PMLSM) is an optimal driving source in a linear motion system such as a machine tool, an industrial machine, an OA machine and etc.. Especially, the slotless type PMLSM has disadvantage of low power density because magnetic air-gap is large. But, the slotless type PMLSM does not generate detent force caused by the structure of slot-teeth. Thus it has not only no thrust ripple but also low normal force. Therefore, it is suitable to apply the slotless type PMLSM to the machines that need precise controllability [1,2]. Nowadays, the interest in slotless type PMLSM is increasing with energy density.

Therefore, in this paper, in order to improve low thrust density that is the biggest disadvantage of slotless type PMLSM, optimal design is performed. As the characteristic analysis technique, the 3-dimensional space harmonic method is used to reduce the analysis time of characteristics with the change of parameters and to illustrate accurately the configuration of the end part of armature coil.

If the space harmonic method is used to analysis of slotless type PMLSM, the result of Finite Element Analysis was not different. Because the slotless type PMLSM has a simple structure and it has no magnetic saturation of core.

The optimal design was achieved by combining a genetic algorithm with the 3-dimensional space harmonic method in order to improve thrust[3].

* The authors are with the Electrical Engineering Department, Changwon National University, Chang-won, Gyeong-nam, Korea.
(dongyeuplee@changwon.ac.kr, gtkim@sarim.changwon.ac.kr)
Received June 7, 2005 ; Accepted August 23, 2005

2. Slotless type PMLSM

Prototype machine is shown in Fig. 1. As shown in Fig.1, magnetic saturation of iron core is not generated in the slotless type PMLSM because of large magnetic air-gap. And also the structure is simple.

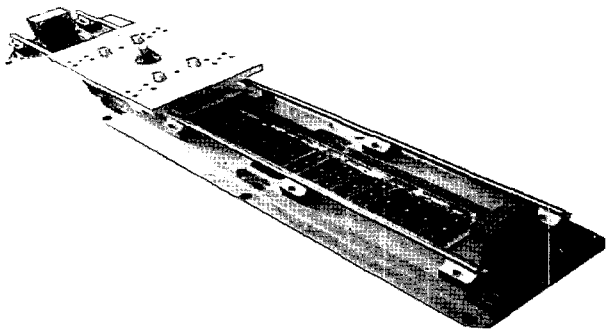

Fig. 1 Prototype machine

Accordingly, the result of characteristic analysis using an analytical method such as space harmonic method is similar to the result of FEM considering with saturation of core.

Table 1 dimension and specification of analysis model

Parameter	Values	Parameter	Values]
Number of poles	12	Turns per phase	650 [turns]
Residual induction	1.2 [T]	Height of winding	11 [mm]
Height of PM	12 [mm]	Width of winding	12 [mm]
Length of PM	73.5 [mm]	Distance of windings	12 [mm]
Width of PM	26 [mm]	Phase current(max)	2.66 [A]
Pole pitch	28.5 [mm]	Length of air-gap	2 [mm]

Also, because air gap magnetic reluctance is regular, detent force is not generated due to the dispersion of air gap magnetic reluctance. Normal force generated as the reluctance in driving is 7~8 times smaller than one of slot type PMLSM. Therefore, the slotless type PMLSM is suitable to be applied to machines that need precise controllability [1].

3. 3 Dimension space harmonic method

3.1 Magnetic field of PM

This paper uses the magnetic scalar potential φ in magnetic field calculation and Fig. 2 shows magnetization distribution. And this paper assumes that magnetization is uniform in the y-axis direction.

$$\overline{M} = M_x\overline{a_x} + M_y\overline{a_y} + M_z\overline{a_z} \tag{1}$$

This magnetization distribution is represented as equation (2) using Fourier series.

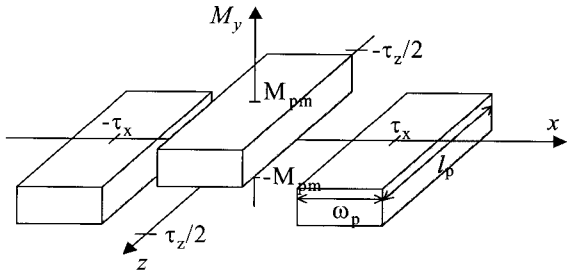

Fig. 2 Magnetization distribution by PM

$$M_y = \sum_{m=1}^{\infty}\sum_{n=1}^{\infty} M_{mn}\cos(mk_x x)\cos(nk_z z) \tag{2}$$

where, k_x is π/τ_x, and k_z is π/τ_z.

M_{mn} is given by

$$M_{mn} = \frac{16M_{pm}}{mn\pi^2}\sin(m\alpha_x\frac{\pi}{2})\sin(n\alpha_z\frac{\pi}{2}) \quad (m,n = 1,3,5,...) \tag{3}$$

where, α_x is w_p/τ_x, α_z is l_p/τ_z, w_p is the width of PM, l_p is the length of PM, τ_x is pole pitch for x-axis direction, and τ_z is pole pitch for z-axis direction.

Meanwhile, equations (4) and (5) are governing equations in the air and permanent magnet region, respectively.

$$\nabla^2\varphi_I^{pm} = 0 \quad \text{(In air gap region)} \tag{4}$$

$$\nabla^2\varphi_{II}^{pm} = \frac{\nabla\cdot\bar{M}_y}{\mu_r} = 0 \quad \text{(In PM region)} \tag{5}$$

From the general solution of equations (4) and (5) and boundary condition, the air-gap flux density can be written in the following form:

$$B_{xI}^{pm} = -\sum_{m=1,3,...}^{\infty}\sum_{n=1,3,...}^{\infty}\frac{mk_x}{k_{mn}}\beta_m\sinh(k_{mn}y)\cdot\sin(mk_x x)\cos(nk_z z)$$

$$B_{yI}^{pm} = +\sum_{m=1,3,...}^{\infty}\sum_{n=1,3,...}^{\infty}\beta_m\cosh(k_{mn}y)\cos(mk_x x)\cdot\cos(nk_z z)$$

$$B_{zI}^{pm} = -\sum_{m=1,3,...}^{\infty}\sum_{n=1,3,...}^{\infty}\frac{nk_z}{k_{mn}}\beta_m\sinh(k_{mn}y)\cdot\cos(mk_x x)\sin(nk_z z)$$

where β_m is given by

$$\beta_m = \frac{\mu_0 M_{mn}\sinh(k_{mn}(y_m - y_s))}{\xi_m}$$

$$\xi_m = \mu_r\cosh(k_{mn}y_m)\sinh(k_{mn}(y_m - y_s)) - \cosh(k_{mn}(y_m - y_s))\sinh(k_{mn}y_m)$$

3.2 Magnetic field of armature current

The 3-dimensional field distribution of current calculation is more difficult than that of PM because of the shape of end-coil with half-circle configuration. Thus, in this paper, the shape is assumed to be rectangular as shown in Fig. 3.

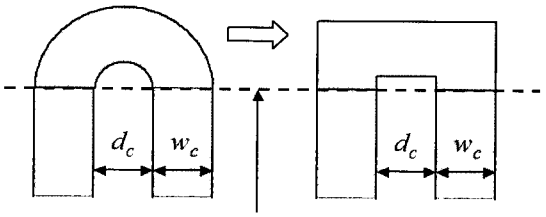

Fig. 3 Equivalence of end-coil

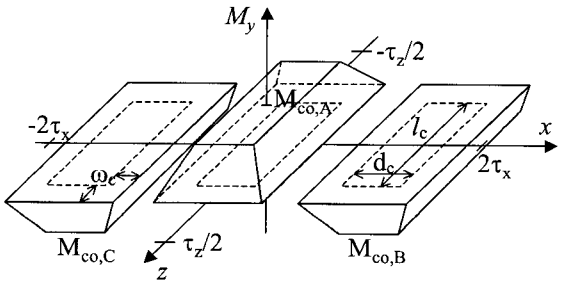

Fig. 4 Magnetization distribution by armature current

The magnetization of armature current that has rectangular shape end-coil can be expressed as shown in Fig. 4. The magnetization distribution of armature current is similar to that of PM, so the distribution can be represented as equation (3), and Fourier's coefficient M_{mn} can be written in the following form:

$$M_{mn} = \frac{32M_{co}}{m^2n^2\pi^2}\frac{1}{k_x k_z w_c^2}\sin(mk_x\frac{d_c+w_c}{2})\sin(mk_x\frac{w_c}{2}) \cdot\sin(nk_z\frac{l_c+w_c}{2})\sin(nk_z\frac{w_c}{2}) \quad (m=1,2,3,\ldots\ n=1,3,5,\ldots) \tag{6}$$

Using the same process of PM, flux density can be calculated.

Fig. 5 shows the magnetic field distribution by PM and armature current.

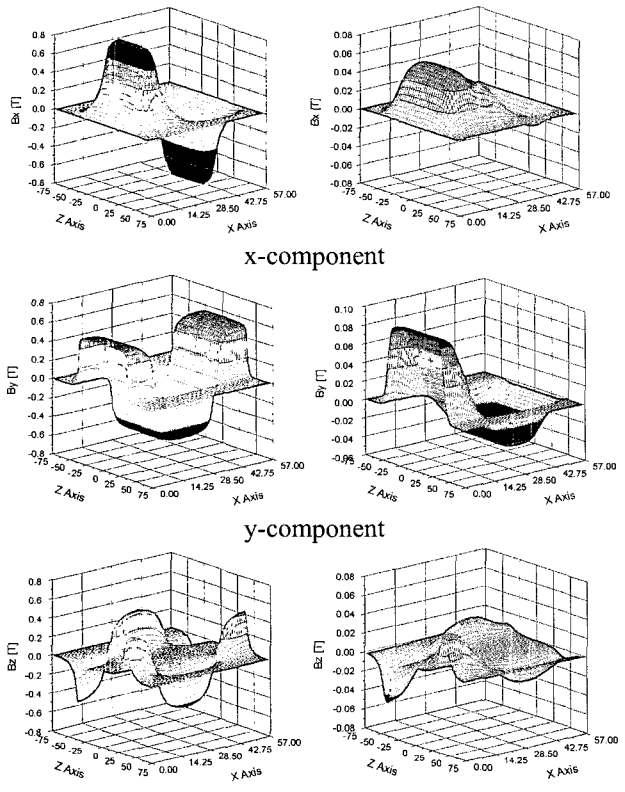

x-component

y-component

z-component

(a) air-gap field by PM (b) air-gap field by current

Fig. 5 Magnetic field distribution at the air-gap

3.3 Characteristic analysis

Thrust can be calculated using Maxwell stress tensor method. Fig. 6 shows thrust according to displacement. The result obtained by 3-D space harmonic was appeared smaller than the result of FEM by about 3.26[%]. It was a good result harmonized with the experiment value.

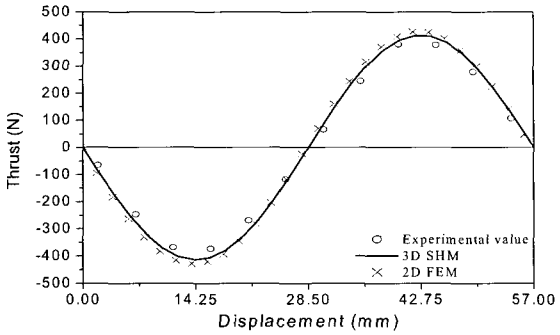

Fig. 6 Thrust according to displacement

4. optimization of slotless type pmslm

In engineering problems with many minimum solutions, the techniques of probability theory are widely used in such a genetic algorithm, as the method of finding the minimum point. Therefore, this paper used genetic algorithm with MATLAB and applied to the optimization of slotless type PMLSM.

4.1 Selection of design variables and restricted conditions

The optimal design was achieved by combining a genetic algorithm with the space harmonic method in order to improve thrust[3].

As shown Fig. 7, the width permanent magnet (w_p), the thickness of permanent magnet (h_p), the width of coil (w_c), the distance between coils (d_c) and the length of core lamination direction (L_z) are selected as design variables.

If the length of core lamination is increased, the thrust is also improved. So, the functional was set as thrust per weight, thrust per volume and multi-objective function in which the combination of thrust per weight and thrust per volume has the ratio of 1:1.

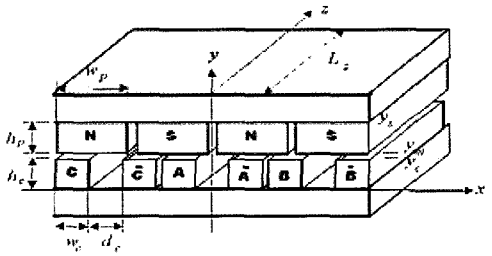

Fig. 7 Design parameter

$$F_x = F_L + m\frac{dv}{dt} + Dv \tag{7}$$

Equation (7) is a kinetic equation in which F_x is thrust, F_L is load thrust, M is load mass, D is friction coefficient,

and v is velocity. In this part, load thrust is 250[N], the weight of mover is 10[kg]. So, the thrust considering friction force is calculated. The result is about 450[N]. Therefore, in this paper, thrust was set between 447.25[N] and 452.75[N] as a constrained condition.

Table 2 Design variables and constrained conditions

Design variables	Range
w_p	$24[mm] \leq w_p \leq 28[mm]$
w_c	$8[mm] \leq w_c \leq 16[mm]$
d_c	$3[mm] \leq d_c \leq 16[mm]$
L_z	$66[mm] \leq L_z \leq 80[mm]$
Constrained conditions	$447.25[N] \leq thrust \leq 452.75[N]$
	Distortion ratio $\leq 0.5[\%]$

4.2 The flow chart of genetic algorithm

Fig. 8 shows the flow chart of genetic algorithm. After the design variables are converted to 2-string and mixing, initial population is randomly generated. The roulette wheel selection is used for reproduction.

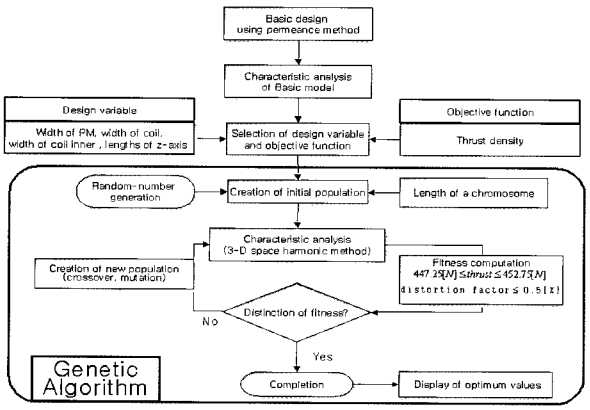

Fig. 8 The flow chart of genetic algorithm

4.3 Optimization result

Fig. 9 is shown the optimization procedure of multi-objective functions using a genetic algorithm. Table Ⅲ. shows the specifications and result of optimization for each objective function. In case of optimization with an objective function using thrust/weight, thrust/weight was increased 10.87[%] but thrust/volume was increased 4.93 [%], comparing with a prototype machine. Also, in case of optimization with an objective function using thrust/volume, thrust/volume increased 13.1[%] but thrust/weight increased only 4.96 [%], comparing with prototype machine. In case of optimization as multi-objective functions, thrust/weight has increased 7.56[%] and thrust/volume increased 7.98[%], comparing with the prototype machine.

Therefore, this result is satisfied with not only in the side of miniaturization but also in the side of lightweight.

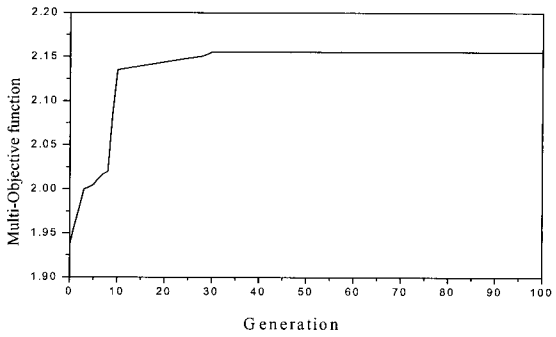

Fig. 9 Optimization procedure of multi-objective functions

Table 3 Analysis results by neural network

	Prototype machine	Max. Thrust per Weight	Max. Thrust per Volume	Multi-objective functions
Wp [mm]	26	24.3	28	26.3
Lz [mm]	73.5	76.5	70	73.5
Wc [mm]	12	16	15.5	16
Dc [mm]	12	5	5.5	4
Thrust[N]	417.434	451.8	448.2	450.716
Thrust/weight	0.115	0.1275	0.1207	0.1237
Thrust/volume	2.229	2.339	2.521	2.407

4.4 Characteristic analysis

As shown in Fig. 10, as the result of analyzing the harmonic component of thrust, in the case of the selecting the objective function as thrust/weight having the maximum distortion ratio, the distortion ratio is 0.22 [%] and then satisfactory design has been progressed.

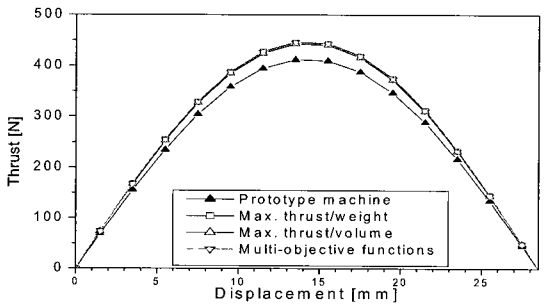

(a) Thrust

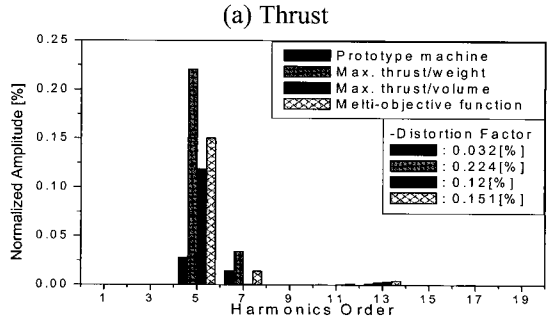

(b) Harmonic component

Fig. 10 The characteristic analysis

Fig. 11 shows the characteristics of thrust upon steady states operation for a prototype machine and an optimal model in load angle of 60 degree. The thrust ripple is increased in the optimal model comparing to prototype machine. But, In the case of selecting thrust/weight model having the biggest thrust ripple as an objective function, peak to peak value of thrust ripple is about 2.5[N]. Because ripple ratio is 0.67[%], it doesn't influence on the change of control ability.

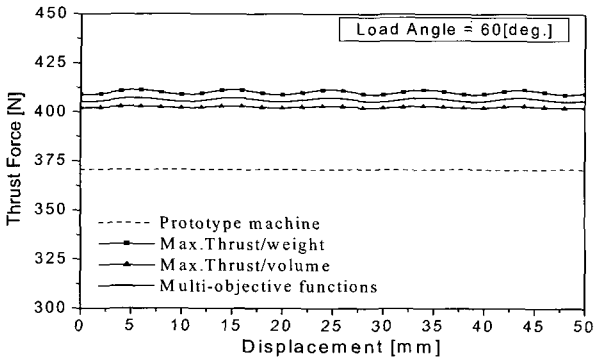

Fig. 11 Thrust of slotless type PMLSM in steady state operation

5. Conclusion

In this paper, 3D space harmonic method is applied to characteristic analysis in a slotless type PMLSM with high control ability and then optimal design was achieved by using a genetic algorithm. The characteristic analysis using 3- dimensional space harmonic method resulted in an exact solution without any error, comparing to the experiment value. Using the genetic algorithm with the 3D space harmonic method reduces the processing time in optimization. In case of optimization using multi-objective functions, thrust/weight has increased 7.56[%] and thrust/ volume increased 7.98[%], comparing with the prototype machine.

Therefore this result is satisfied with not only in the side of miniaturization but also in the side of lightweight.

References

[1] Jacek F. Gieras, Zbigniew J. Piech, Linear Synchronous Motors - Transportation and Automation Systems, CRC Press, 2000.

[2] Ki-Chae Lim, Jung-Pyo Hong, Gyu-Tak Kim, "The Novel Technique Considering Slot Effect by Equivalent Magnetizing Current", IEEE Trans. on Magnetics, Vol. 35, No. 5, pp. 3691-3693, 1999.

[3] Sang-Yong Jung, Jae-Kwang Kim, Hyun-Kyo Jung, Cheol-Gyun Lee, Sun-ki Hong, "Size Optimization of Steel-Cored PMLSM Aimed for Rapid and Smooth Driving on Short Reciprocating Trajectory Using Auto-Tunig Niching Genentic Algorithm", IEEE Trans. on Magnetics, Vol. 40, No. 2, pp. 750-753, 2004.